Journal of Environmental Management 220 (2018) 233–245

Contents lists available at ScienceDirect

Journal of Environmental Management

journal homepage: www.elsevier.com/locate/jenvman

Research article

Evaluating long-term patterns of decreasing groundwater discharge through a lake-bottom permeable reactive barrier

Timothy D. McCobb [a, *], Martin A. Briggs [b], Denis R. LeBlanc [a], Frederick D. Day-Lewis [b], Carole D. Johnson [b]

[a] U.S. Geological Survey, 10 Bearfoot Road, Northborough, MA, 01532, USA
[b] U.S. Geological Survey, Earth Systems Processes Division, Hydrogeophysics Branch, 11 Sherman Place, Unit 5015, Storrs, CT, 06269, USA

ARTICLE INFO

Article history:
Received 6 December 2017
Accepted 23 February 2018
Available online 21 May 2018

Keywords:
Groundwater/surface-water interaction
Permeable reactive barrier (PRB)
Instruments and techniques: monitoring
Instruments and techniques: modeling
Fiber-optic distributed temperature sensing (FO-DTS)
Temperature

ABSTRACT

Identifying and quantifying groundwater exchange is critical when considering contaminant fate and transport at the groundwater/surface-water interface. In this paper, areally distributed temperature and point seepage measurements are used to efficiently assess spatial and temporal groundwater discharge patterns through a glacial-kettle lakebed area containing a zero-valent iron permeable reactive barrier (PRB). Concern was that the PRB was becoming less permeable with time owing to biogeochemical processes within the PRB. Patterns of groundwater discharge over an 8-year period were examined using fiber-optic distributed temperature sensing (FO-DTS) and snapshot-in-time point measurements of temperature. The resulting thermal maps show complex and uneven distributions of temperatures across the lakebed and highlight zones of rapid seepage near the shoreline and along the outer boundaries of the PRB. Repeated thermal mapping indicates an increase in lakebed temperatures over time at periods of similar stage and surface-water temperature. Flux rates in six seepage meters permanently installed on the lakebed in the PRB area decreased on average by 0.021 md^{-1} (or about 4.5 percent) annually between 2004 and 2015. Modeling of diurnal temperature signals from shallow vertical profiles yielded mean flux values ranging from 0.39 to 1.15 md^{-1}, with stronger fluxes generally related to colder lakebed temperatures. The combination of an increase in lakebed temperatures, declines in direct seepage, and observations of increased cementation of the lakebed surface provide in situ evidence that the permeability of the PRB is declining. The presence of temporally persistent rapid seepage zones is also discussed.

Published by Elsevier Ltd.

1. Introduction

Understanding groundwater exchange at the groundwater/surface water (GW/SW) interface is essential for characterizing the fate and transport of contaminants. The heterogeneous nature of stream and lakebed sediments can result in a highly variable distribution of areal fluid flux across this interface (Kamolpornwijit et al., 2003; Kazmierczak et al., 2016; Rosenberry et al., 2016, 2015). Whereas groundwater-contaminant concentrations (mass per volume) below a lakebed can be obtained with spatially dense sampling techniques, estimates of mass-contaminant flux (mass per time) require spatially detailed fluid flux estimates which can be difficult to quantify. For example, nutrient inputs from groundwater to lakes and ponds at low-to-moderate concentrations can lead to concerns over eutrophication if those inputs enter in areas of high groundwater flux. Significant total constituent loading to receiving waters can occur that would not reflect the concentrations at the limited point scale. Even with the recent development of new measurement technologies, quantifying accurate spatiotemporal groundwater discharge patterns is difficult, and examples of field examinations over large areas and longer timeframes are limited. The assessment of risk to the ecological health of a receiving water body relies strongly on the information regarding groundwater fluxes in systems, which are too often based on sparse point-in-time measurements.

In zones of persistent groundwater contamination, mass loading of surface-water bodies can be initially decreased through the installation of in situ permeable reactive barriers (PRB) that intercept and alter the chemistry of discharging flowpaths. PRBs are an

* Corresponding author.
E-mail address: tmccobb@usgs.gov (T.D. McCobb).

https://doi.org/10.1016/j.jenvman.2018.02.083
0301-4797/Published by Elsevier Ltd.

innovative groundwater remediation technology that uses reactive material placed along a groundwater flowpath to passively remediate contaminated groundwater through sorption, precipitation, reaction, and biodegradation processes. Common materials used for PRBs include zerovalent iron (ZVI), biological barriers, surfactant-modified zeolites, and peat moss. However, long-term monitoring of such remediation solutions is typically not systematic and spatially distributed, even though PRBs are expected to decrease in efficacy over time. For example, laboratory and numerical simulation have shown strong potential for PRB clogging or reduced permeability from mineral precipitation and biogeochemical changes as a PRB ages (Gu et al., 1999; Kamolpornwijit et al., 2003; Li et al., 2005; Liang et al., 2003; Su and Puls, 2003). Reduced permeability from corrosion and mineral precipitation can lead to reduced treatment effectiveness by decreasing hydraulic residence times (via focused discharge) and total flow though the PRB (Sass et al., 1998). Hydraulic bypassing or short circuiting can occur where preferential flow paths follow more permeable zones outside of the barrier. Few field examples of sufficient duration and consistent methodology are documented in the literature about PRB performance issues over time owing to the difficulty of monitoring flow characteristics through PRBs, which are typically installed vertically at depth in an aquifer. Examining sediment cores, Phillips et al. (2010) reported restricted groundwater flow thorough a ZVI PRB, likely by mineral precipitation and ZVI filings clumping together through cementation. Wilkin et al. (2003) documented reductions in porosity ranging between 0.032 and 0.062 by using multiple cores at two PRBs after only 4 years. Limited documentation is published on the long-term performance of horizontal reactive barriers installed more recently at the shores of lakes, ponds, and coastal estuaries.

Traditional field methods to examine and quantify groundwater exchange at many scales across the interface include direct point measurements of water flux by using physical seepage meters (Lee, 1977; Lee and Cherry, 1978; Carr and Winter 1980; Murdoch and Kelly, 2003; Rosenberry and Morin, 2004; Rosenberry et al., 2016), Darcian methods utilizing hydraulic head and hydraulic conductivity from field measurements to estimate vertical specific discharge (e.g. Rosenberry and LaBaugh, 2008), water and chemical budget approaches such as differential stream gaging and chemical tracer tests in streams (e.g. Harvey et al., 1996) and the segmented-lake budget method (e.g. Healy et al., 2007), and the use of heat as a tracer of water flow (Anderson, 2005; Constantz et al., 2003). In recent years, heat-based methods have become more routine, yielding great advances in both temperature measurement techniques and simulation of coupled heat and water transport as documented by many review papers (Anderson, 2005; Constantz, 2008; Irvine et al., 2017b; Stonestrom and Constantz, 2003). Temperature is a relatively easy, inexpensive, and robust parameter to measure, making it an attractive approach for groundwater discharge field investigations (Kalbus et al., 2006). In general, the use of temperature as a tracer relies on differences in groundwater and surface-water temperatures to spatially identify areas of GW/SW exchange, while vertical thermal profiles in bed materials are used to model exchange rates (Rau et al., 2014).

Thermal mapping of spatial thermal patterns at or near the bed interface to indicate the distribution of groundwater discharge has been applied in fluvial settings by using many different methodologies. Snapshot-in-time (S-I-T) measurements of temperature, collected over short time intervals (hour scale), utilize a temperature probe inserted into the bed sediment to a given depth to delineate patterns in temperature differences between surface water and sub-bottom groundwater (e.g. Conant, 2004; Gordon et al., 2013; Irvine and Lautz, 2015; Lautz and Ribaudo, 2012). The sub-bottom temperatures are governed by heat conduction between surface water and groundwater and vertical heat advection of surface or groundwater (Conant, 2004). Collection of data within the subsurface (rather than on the interface itself) can amplify spatial variability in thermal signals resulting from preferential flow and reduce the effect of differential solar heating. In advection-dominated discharge zones, sub-bottom temperatures more closely reflect the relatively stable deeper groundwater temperature; in conduction-dominated zones, sub-bottom temperatures closely track the surface-water temperature (Stonestrom and Constantz, 2003). Contrasts in temperature can be used to identify exchange zones and vary as temperatures change daily and seasonally (Conant, 2004; Lautz and Ribaudo, 2012).

Groundwater studies have used fiber-optic distributed temperature sensing (FO-DTS) to characterize exchange with surface water (Selker et al., 2006). The technology is based on the evaluation of laser-light backscatter that occurs as light travels along optic fibers to provide high spatial resolution (typically 0.125–2m), real-time monitoring of temperature along the entire length of a cable (Tyler et al., 2009). FO-DTS has been used as a tool to spatially identify and characterize seepage zones in fluvial, lacustrine, and estuarine settings (Selker et al., 2006; Westhoff et al., 2007; Lowry et al., 2007; Henderson et al., 2009; Slater et al., 2010; Sebok et al., 2013), applied vertically at the GW/SW interface (Briggs et al., 2016, 2012; Mamer and Lowry, 2013), and in fractured rock boreholes to assess vertical water movement (Read et al., 2013; Banks et al., 2014).

Vertical groundwater flux at the GW/SW interface can be quantified by numerical and analytical modeling of depth profiles of temperature under a variety of configurations (Irvine et al., 2017a; Rau et al., 2010). Numerical models that solve the flow and heat-transport equations in porous media, such as VS2DH (Healy and Ronan, 1996; Koch et al., 2016) and SUTRA (Voss, 1984), have been developed to solve coupled flow and heat transport problems. Signal-based analytical solutions utilize diurnal signal amplitude ratio and/or phase lag characteristics between two depths to quantify vertical fluid flux (Bredehoeft and Papadopulos, 1965; Carslaw and Jaeger, 1959; Goto et al., 2005; Hatch et al., 2006). Recent work has shown that amplitude ratio-based analytical models in particular can yield vertical groundwater flux information that is similar to that obtained from numerical models (e.g. Briggs et al., 2014) and physical seepage meters (e.g. Rosenberry et al., 2016), at sub-daily temporal resolution over extended periods.

The purpose of this study was to assess long-term hydrologic changes at a passive ZVI PRB installed on a lakebed to intercept a known phosphate plume in groundwater at its discharge point under natural gradient conditions. Here we examine indicators of long-term water fluxes over multiple years through the lakebed PRB by using repeatable, inexpensive, robust, and time-efficient monitoring techniques and relate them to PRB performance. The paper will discuss hydrologic implications for contaminant treatment, indications of PRB clogging, and the presence of persistent focused groundwater discharge zones.

2. Site description and hydrologic setting

Patterns of groundwater discharge over 11 years were examined at a lake-bottom ZVI PRB installed to intercept a discharging phosphate plume originating from upgradient wastewater infiltration beds (McCobb et al., 2009a). An ongoing concern that is typical of most ZVI PRB sites is that the PRB is becoming less permeable with time owing to biogeochemical processes related to iron oxidation and formation of iron-phosphate minerals and, therefore, less effective at removing phosphate from groundwater discharging to the lake. The PRB covers 1100 m^2 of lakebed along

91 m of the shoreline of Ashumet Pond, a glacial kettle lake located in Falmouth, Mass., on western Cape Cod (Fig. 1). The PRB, installed in October 2004, consists of 30 tons of granular ZVI mixed into ambient lakebed material to a depth of about 0.75 m. The geochemical design life of the PRB is 20 years given measured phosphate concentrations and expected discharge rates (McCobb et al., 2009a, 2003). The bed materials consist of poorly sorted fine to medium sands with some cobbles. Most cobbles in the PRB area were removed from the matrix during the installation mixing process. Previous direct point-scale measurements of seepage in the area ranged from 0.003 to 0.967 md^{-1} (Air Force Center for Environmental Excellence, 1997; McCobb et al., 2009a; Rosenberry et al., 2013; Rosenberry and Morin, 2004). McCobb et al. (2009a) reported differences in mean seepage flux from paired meters spaced less than 1 m apart ranging from 0.003 to 0.455 md^{-1}, with a mean difference of 0.146 md^{-1} indicating strong influence of near-surface heterogeneity on discharge rates.

Groundwater in the treatment zone of the PRB is geochemically characterized as suboxic to anoxic, with greatly elevated specific conductance, pH, and dissolved iron, relative to background groundwater and the lake water (McCobb et al., 2009b). Spatial snapshots of concentration obtained by using temporary well points have shown that the PRB is effective at removing phosphate, although the effectiveness varies with pond stage, with less removal at periods of higher stage when the plume discharges landward of the PRB boundary near the shoreline where water flux rates are typically greatest (McCobb et al., 2009b).

3. Methods

A toolbox approach of comprehensive lakebed temperature mapping and point-scale measurements of seepage flux was used to examine spatial and temporal seepage patterns in the area of the lakebed PRB. Four methods were employed in this work—fiber-

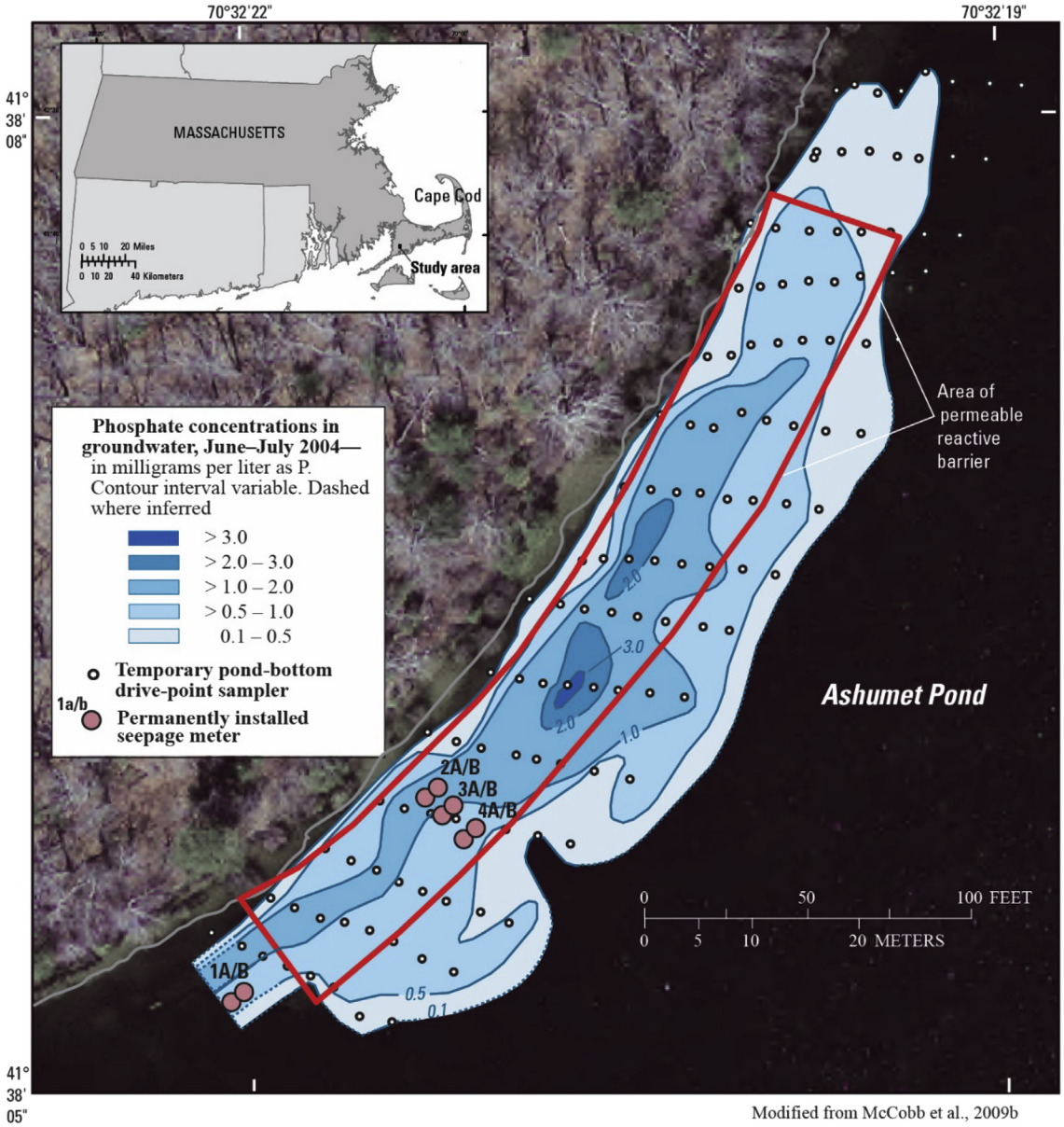

Fig. 1. Areal distribution of phosphate concentrations in lake-bottom groundwater prior to installation of a permeable reactive barrier, July 2004, Ashumet Pond, Cape Cod, Massachusetts.

optic distributed temperature sensing, snapshot-in-time temperature measurements, seepage meters, and vertical temperature profilers. The application of each technique is described in detail below. Although the techniques for evaluating PRB efficacy were not applied concurrently for the period of evaluation, the methods are comparable and provide a robust examination of spatial and temporal seepage patterns near the lakebed PRB.

3.1. Nearshore lakebed temperature using fiber-optic distributed temperature sensing

The distribution of lakebed temperatures was determined over an 18-hour period in May 2007, 2.4 years after PRB installation, by using a LIOS FO-DTS system (LIOS Technology, Cologne, Germany, model 2000/4000) connected to a 1000-m-long tight-buffered, flexible military-tactical fiber-optic cable (AFL, a subsidiary of Fujikura Ltd., Japan) with aramid for tensile strength and a polyurethane jacket. The FO-DTS system measures temperature by means of optical fibers that function as linear sensors of temperature-dependent laser light backscatter, producing temperature values to an accuracy of ~0.1 °C over each 1-m length of cable. In this application, the cable was deployed using a boat in a zig-zag pattern over the PRB area. Divers used weights to ensure that the cable was flush against the lakebed. The configuration produced temperatures (n = 491) for each minute of deployment. Measurements were performed in single-ended mode, where light is transmitted in only one direction along the cable. The cable was tested and georeferenced using an ice bath, and the position of each vertex of the layout was determined using a handheld Trimble GeoXT GPS unit to submeter accuracy (Trimble Inc., Sunnyvale, CA). Hobo Tidbit temperature loggers (Onset Computer Corp., Bourne, MA, part no. UTBI-001) spaced along the cable provided verification of FO-DTS readings. The FO-DTS survey occurred in late spring during above average stage level (14.11 m) and the mean surface-water temperature was cooler relative to later summer months. Hobo temperature/light data loggers (Onset Computer Corp., Bourne, MA, part no. UA-002-08) recorded surface-water temperatures and light intensity to monitor potential solar heating at 5-min intervals at a site located 20 m from shore and 10 cm above the lakebed over the 18-hr measurement period (Fig. 2B).

3.2. Snapshot-in-time measurements of groundwater temperature below lakebed

Snapshot-in-time temperature measurements at 10 cm below the lakebed in and around the area of the PRB were made using a T-type thermocouple probe (Omega Engineering, Norwalk, CT, part no. THSS-14U-RSC-6) affixed to a rigid PVC rod and handheld thermometer (Cole Parmer, Vernon Hills, IL, part no. EW-91100-20). The measurements were made during the early hours of two consecutive mornings on July 29–30, 2008, August 7–8, 2014, and August 19–20, 2015 between sunrise and 0930, during periods of no precipitation and minimal wind. In 2008 and 2014, point temperature measurement locations (n = 417 and n = 329, respectively) were determined by using the handheld GPS. In 2015, point temperature measurement locations (n = 326) were recorded with a Nikon Nivo 5.M Total Station (Nikon Corporation, Tokyo, Japan) to greater than 3-mm accuracy. The lake shoreline position of each event was also recorded using handheld GPS, and all surveys included readings at permanent lakeshore monuments set up for the duration of the study to ensure positioning between surveys was directly comparable.

Temperature snapshots for each measurement period were collected during periods of similar pond stage (13.64 m, 13.56 m, and 13.51 m, respectively; site no. 413758070320501 at https://nwis.waterdata.usgs.gov) and at similarly warm mean surface-water temperatures relative to groundwater (26.0 °C, 23.3 °C, 26.7 °C, respectively). Background groundwater temperature immediately upgradient of the lake in a well screen 1.5 m below the water table was steady at approximately 10 °C (Savoie et al., 2012, Fig. 1), which is about the local mean annual air temperature. Repeated measurements at control sites during each event showed

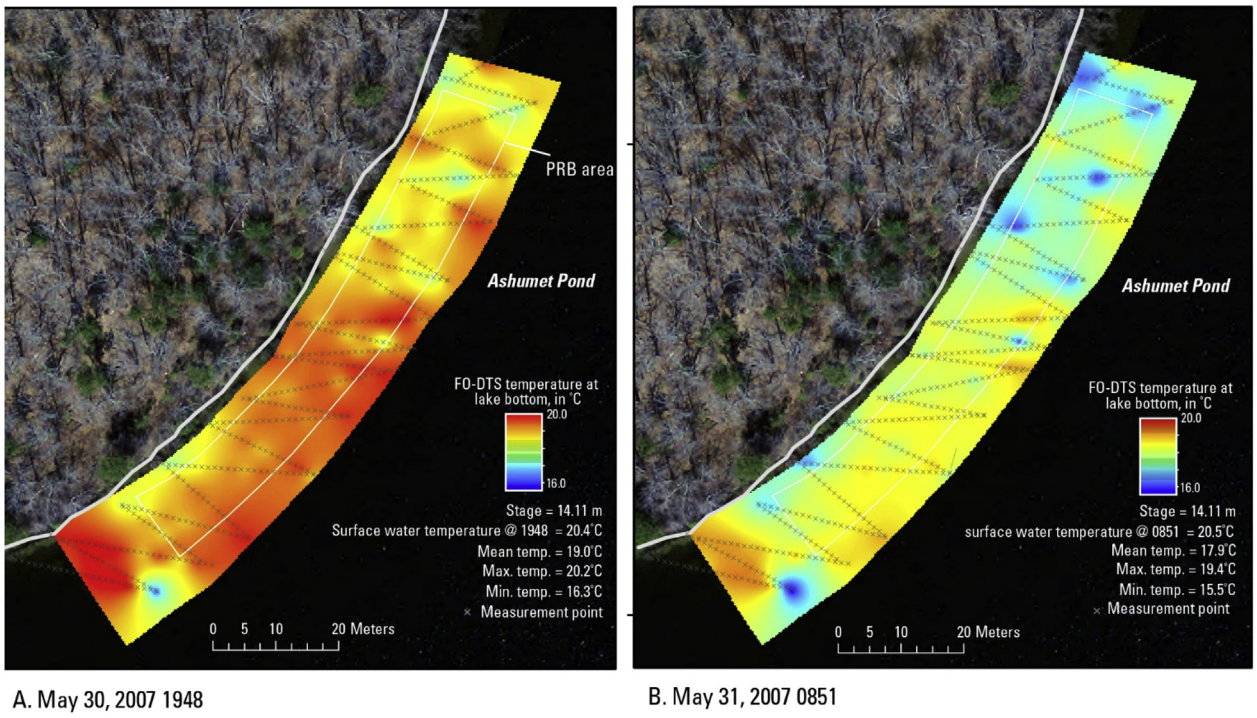

Fig. 2. Lake-bottom temperature determined using fiber optic distributed temperature sensing for evening and morning measurement snapshots, May 30–31, 2007.

slight daily increases in surface-water temperature (mean + 0.96 °C) and lakebed groundwater temperatures (mean + 1.03 °C) as the surveys progressed through the early mornings owing to solar heating. The target measurement area covered the area inside the PRB and extending 6 m north, 14 m south, and 4.5 m lakeward of the PRB boundary, and from 1.5 to 3.5 m between the PRB and the inter-annual shoreline position.

The S-I-T temperature measurements and the FO-DTS data were interpolated spatially using a built-in algorithm in ArcGIS (ESRI, Redlands, CA) that uses a thin-plate spline interpolation technique (Topo-to-Raster), similar to the method used by Gordon et al. (2013) when evaluating vertical fluid flux around stream restoration structures. To quantify the spatial persistency in observed thermal patterns within the PRB zone across surveys, the correlation between inter-annual temperature patterns was assessed with the Spearman's Rank Correlation Coefficient Test using the CORRCOEF.m Matlab program (freely available from http://numerics.mathdotnet.com).

3.3. Long-term direct measurements of seepage

During backfilling of the PRB material in 2004, three pairs of half-barrel seepage meters with removable lids were emplaced on the lakebed in the PRB area at distances of 1.4, 5.9, and 9.6 m from the shoreward boundary of the PRB (McCobb et al., 2009a). This design allows the lid to be removed between field campaigns so that natural bed evolution within the measured area occurs at the same rates and in the same ways as elsewhere within and beyond the PRB. One pair of meters was installed outside of the southwest boundary of the PRB, 5.5 m from the October 2004 shoreline position (Fig. 1). The meters are a modified version of the design by Lee (1977), and measurements followed practical considerations by Rosenberry and LaBaugh (2008). Each meter consists of a 208-L polyethylene, drum cut to a length of 0.8 m and fitted with a removable 0.56-m-diameter lid. A 1.3-cm-diameter hole was drilled into each lid to allow outflow or inflow to be measured. During installation, the top rim of each barrel was positioned to be at the expected grade after backfilling. Each meter cylinder was completely filled with the ZVI/lakebed mixture. The paired meters are separated by approximately 1 m (McCobb et al., 2009a). Beginning in 2004, direct measurements of seepage were made annually over an 11-year period. The mean seepage rate at each meter was determined from 3 to 5 consecutive measurements made over a 1–2 h period.

3.4. Short-term seepage patterns using vertical temperature profilers

From August 21, 2015 to September 3, 2015, vertical temperature profilers designed to quantify groundwater discharge dynamics were installed at seven locations that generally spanned the range of lakebed temperatures observed during the corresponding snapshot survey. Similar to the design of Briggs et al. (2014), hollow stainless steel pipes (2.5 cm OD) were slotted horizontally to allow installation of iButton thermal data loggers (Maxim Integrated DS1922L, 0.0625 °C precision) protected with waterproof silicone caulking. The temperature profilers were gently tapped into the cobbly bed by first driving and then removing a solid rod to create a guide hole of slightly smaller diameter than the logging devices as demonstrated for coarse-grained streambed material by Gordon et al. (2013). After installation, the thermal loggers were located at 0.01, 0.04, and 0.11 m depths, except at two locations where a 0.07-m depth logger was also included.

The diurnal temperature signal amplitude attenuation-based analytical model that is solved automatically with the VFLUX2 software package (Irvine et al., 2015) was used to resolve vertical groundwater seepage at sub-daily intervals; VFLUX2 is run in the Matlab environment (Mathworks, Natick MA). As described by Irvine et al. (2017b), diurnal signals collected in sediments where the heat transport is dominated by conduction are the most appropriate for measuring saturated thermal diffusivity (K_e), which is the master conductive parameter of the attenuation-based analytical solutions employed by the VFLUX2 program. Because K_e may be anomalously high in sediments with metal oxide deposition, such as that in the area of the PRB, this parameter was measured in situ by using the relation developed by Luce et al. (2013) and included in VFLUX2. The two 4-logger profilers were located in areas shown to be anomalously warm in the 2015 S-I-T bed temperature survey, likely indicating low-flux conditions ideal for K_e evaluation. A representative K_e value was then used to model groundwater seepage over time by using the VFLUX2 "vflux_qar_opt" approach defined by Irvine et al. (2017b) at all temperature profiler locations. For comparison, direct measurements of groundwater seepage were also collected in similar locations as the seven temperature profilers on August 20, 2015, by using temporarily-placed seepage meters following the approach of Lee (1977).

4. Results

The large-area thermal mapping efforts that used FO-DTS and S-I-T thermal-probing methodologies, in combination with direct and modeled seepage fluxes, were examined over multiple years to assess potential hydraulic changes in a lakebed PRB. The datasets produced by these efforts and associated metadata are available in McCobb et al. (2018).

4.1. Thermal mapping of bed temperatures by using fiber-optic distributed temperature sensing

The distribution of the interpolated temperatures from the 2007 FO-DTS deployment revealed much spatial variability over the test area. Fig. 2 shows two snapshot periods during contrasting snapshots of the diurnal signal—at 1948 h on May 30, 2007 (PM) and at 0851 h on May 31, 2007 (AM). Recorded surface-water temperatures for both times differed by only 0.1 °C (mean 20.45 °C), however, the means and ranges of lakebed temperatures varied greatly between the two datasets (Table 1). The difference reflects direct solar warming of the lakebed sediments during the snapshots later in the day as exhibited by the light data recorder that showed greater than twice the maximum light intensity during the PM hours (17,900 lux) than the early AM hours after sunrise (8600 lux).

The two temporal snapshots of interpolated FO-DTS data show complex distributions of temperatures with areas of persistent cold and hot anomalies relative to each dataset's respective mean temperature. These distributions varied both parallel to shore and normal to shore. Generally, the coolest temperatures were detected in the nearest 5 m from the shoreline; however, an exponential increase in temperature with distance from shore, a characteristic commonly used to describe lacustrine groundwater discharge in homogenous systems (McBride and Pfannkuch, 1975), was not clearly evident. Most focused cooler anomalies, presumed to be zones of strong groundwater upwelling, were located throughout the northern third of the study area while the southern PRB zone had a more consistent interface temperature with a few strong cooler patches. Two of these cooler patches, both located about 15 m from shore in the southern and mid-study areas, persisted throughout both snapshots and corresponded with topographic lows in the lakebed surface. Southeast of the PRB, within 15 m from shore, only warm temperatures comparable with the surface-water

Table 1
Information and statistics regarding the lake bottom and lakebed temperature datasets [FO-DTS, fiber-optic distributed temperature sensing; S-I-T, snapshot-in-time; °C, degrees Celsius].

	Statistic	FO-DTS		S-I-T		
		2007 (PM)	2007 (AM)	2008	2014	2015
	Start date	May 30	May 31	July 29–30	August 7–8	August 19–20
	Pond stage (m)	14.11	14.11	13.64	13.56	13.51
	Surface-water temperature (°C)	20.4	20.5	26.0	23.3	26.7
Full study area	Number of snapshot points	491	491	417	329	326
	Maximum temperature (°C)	20.3	19.4	27.0	25.8	27.9
	Minimum temperature (°C)	16.2	15.4	11.9	13.2	13.9
	Range (°C)	4.1	4.0	15.1	12.6	14.0
	Mean temperature (°C)	19.1	18.0	19.9	21.2	22.5
	Standard deviation (°C)	0.67	0.74	2.95	2.44	2.89
PRB area	Number of snapshot points	229	229	196	173	158
	Maximum temperature (°C)	20.0	19.0	27.2	24.8	26.2
	Minimum temperature (°C)	17.1	15.9	11.9	14.5	14.9
	Range (°C)	2.9	3.1	15.3	10.3	11.3
	Mean temperature (°C)	19.0	17.9	19.5	21.4	22.9
	Standard deviation (°C)	0.53	0.58	2.23	1.88	2.27

temperature were detected.

4.2. Thermal mapping of bed temperatures using snapshot-in-time sub-surface probe measurements

Interpolated thermal maps from the earliest (2008) S-I-T measurements of lakebed temperature (10 cm below the lakebed) display many spatial characteristics also shown by the initial FO-DTS survey, most notably the strongest warm zone southwest of the PRB area and the cool anomalies at the lakeward edge of the PRB and in the northern PRB area (Fig. 3). Although the FO-DTS provided high data resolution along linear transects collected simultaneously in time, a higher density of measurement locations throughout the study area was achieved with the S-I-T thermal mapping method. This resulted in an improved spatial definition of groundwater-influenced bed temperature patterns.

In general, consistent features in lakebed groundwater temperatures persisted throughout the 7-year period. Larger, contiguous areas of cool temperatures (<16 °C) were present within the first 3m from shore, particularly in the earliest (2008) snapshot

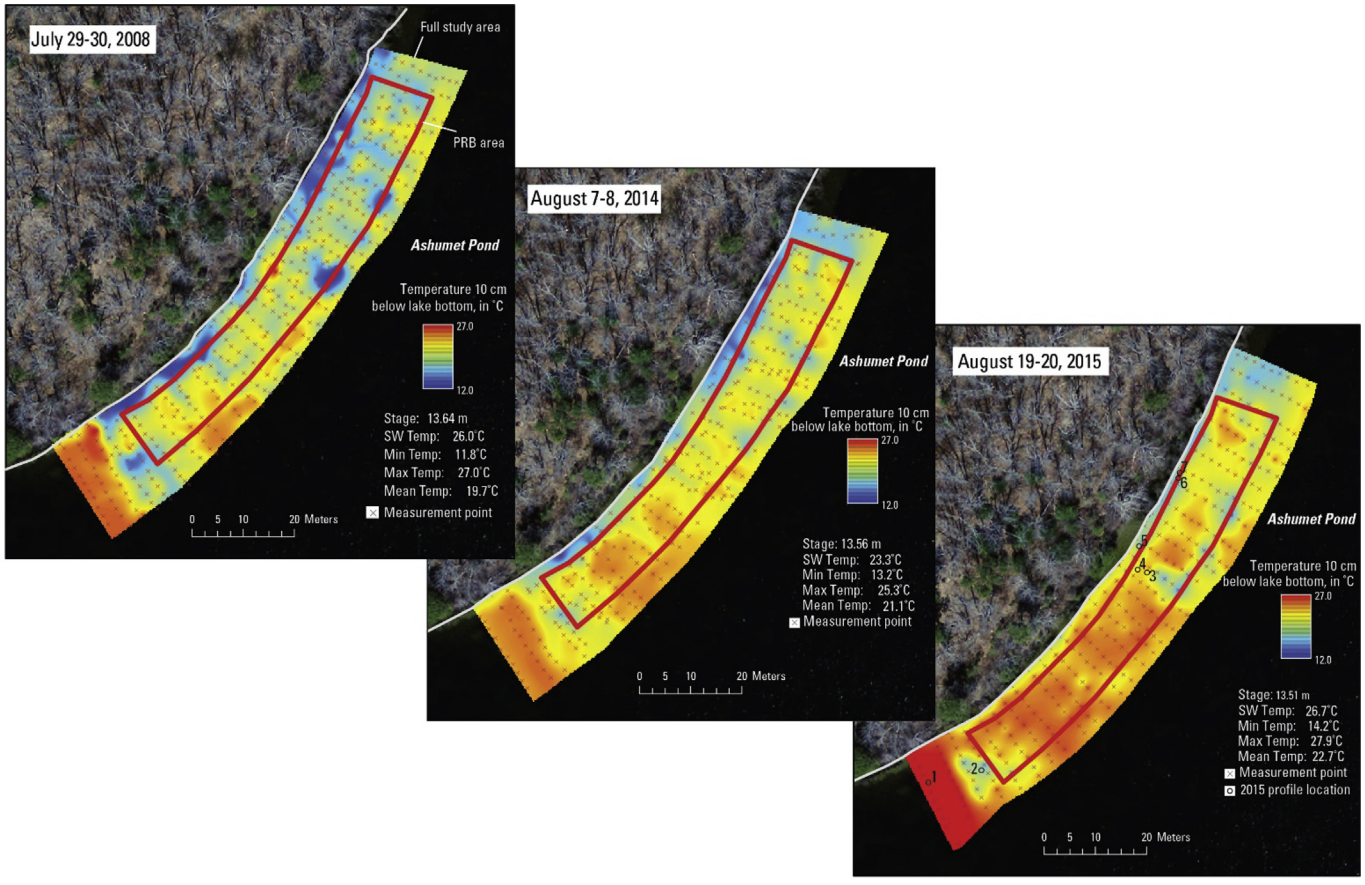

Fig. 3. Lake-bottom temperature determined using fiber optic distributed temperature sensing for evening and morning measurement snapshots, May 30-31, 2007.

Table 2
The Spearman's ranked correlations test between interpolated lakebed thermal maps within the PRB zone.

Year pairing	Correlation coefficient	p value
2008–2014	0.68	<0.01
2008–2015	0.61	<0.01
2014–2015	0.64	<0.01

during the period of highest stage (Table 1). Surprisingly, the coldest temperatures recorded during the 2008 and 2015 snapshots were located offshore along the outer edge of the PRB at locations of topographic lows. For all snapshots, the warmest temperatures, comparable to surface water, occurred in a contiguous area southwest of the PRB extending from the shoreline lakeward to the outer boundary of the study.

The Spearman rank test between each pairing of the three snapshots of interpolated S-I-T lakebed temperatures inside the PRB area shows that the spatial pairings are strongly and positively correlated (Table 2). This confirms the qualitative visual analysis discussed above that relatively warm and cool zones were located in similar PRB regions, indicating control of these patterns by the physical process of groundwater upwelling, rather than simple differential lakebed solar heating. The correlation between the successive survey pairs (2008–2014 and 2014–2015) decreased slightly from 0.68 to 0.64 and was lowest (0.61) when comparing the first and last surveys. The decrease in correlation over time may reflect the effect of clogging processes, particularly in the southern PRB zone where cool anomalies appear to diminish by 2015 (Fig. 3).

Surface-water temperatures for 2008 and 2015 were near an annual high and within a 0.9 °C difference of each other, whereas the 2014 survey occurred at a slightly lower surface temperature, resulting in a smaller range and standard deviation of temperatures for the snapshot (reduced contrast between surface water and groundwater, Table 1). Overall, mean temperatures over both the full study and the PRB-only areas increased with time. Mean temperatures between 2008 and 2015, a period of similar surface-water temperature, in the full study area increased 2.6 °C; inside the PRB mean temperatures increased 3.4 °C.

Comparisons of the spatial characteristics of S-I-T datasets over time are complicated by the differing ranges by year, and particularly the maximum range, which occurs in areas where downward conduction is particularly dominant. To facilitate comparison of spatial and temporal trends between datasets, each S-I-T dataset was normalized to the surface-water temperature at the time of sampling. The normalized thermal maps represent temperature as a scalar of surface-water temperature (0.0–1.0), with low values representing upward advection-dominated zones and values of unity representing zones of thermal conduction (Fig. 4). The normalized thermal maps accentuate the presence of advection-dominated zones nearest the shoreline, along the lakeward PRB boundary, and at both lateral PRB boundaries. The normalized datasets visually show trends in warming over the PRB area over time with a strong decrease in areas of normalized temperatures less than 0.8 inside the PRB area with time, reflective of increasing temperatures. In addition to the increases over the PRB area, temperatures were warmer along the shoreline in 2015, a period when the lake stage was low and the margin between the shoreline and

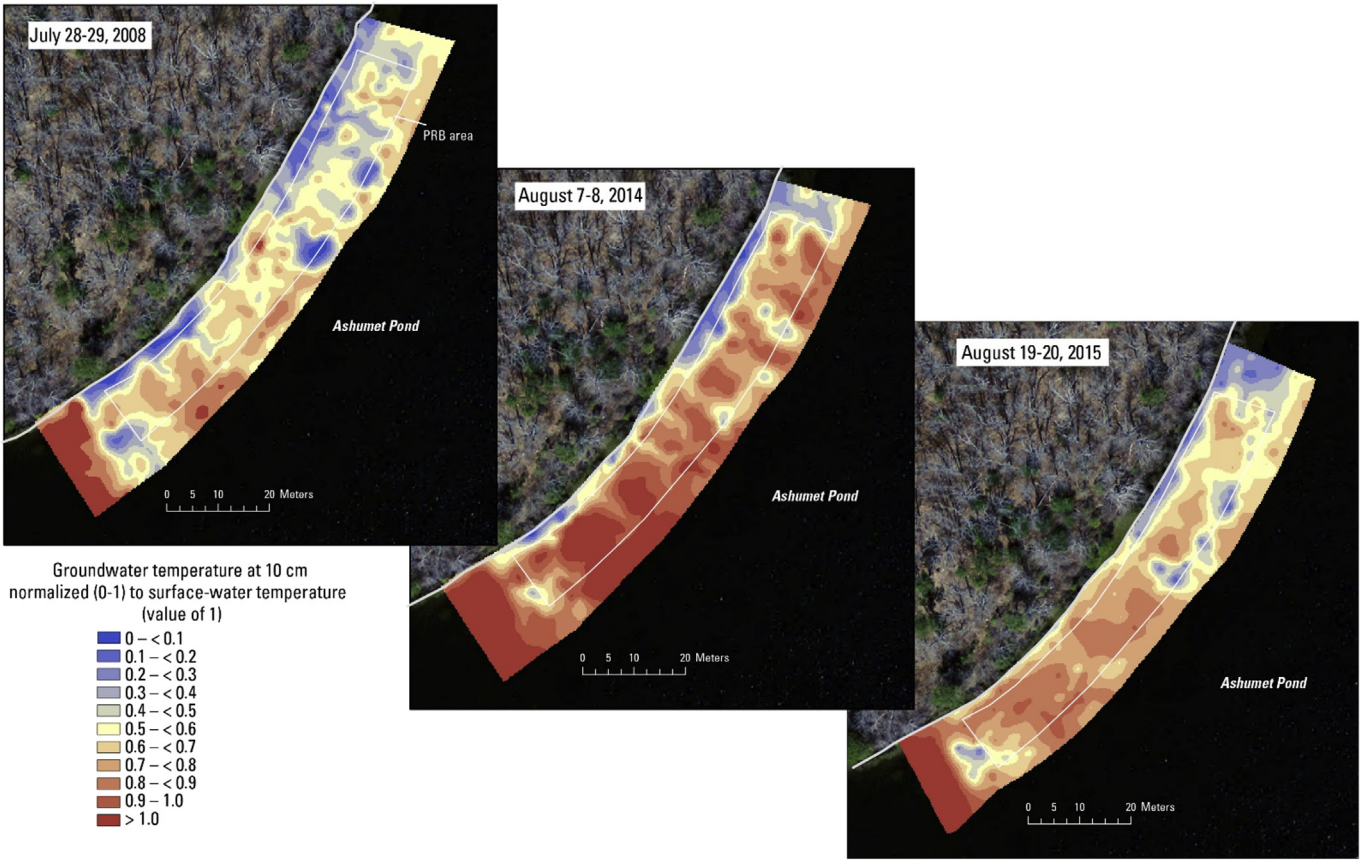

Fig. 4. Maps showing groundwater temperature (10-cm below the lake bottom) normalized to surface water temperature in 2008, 2014, and 2015 in the area of a permeable reactive barrier.

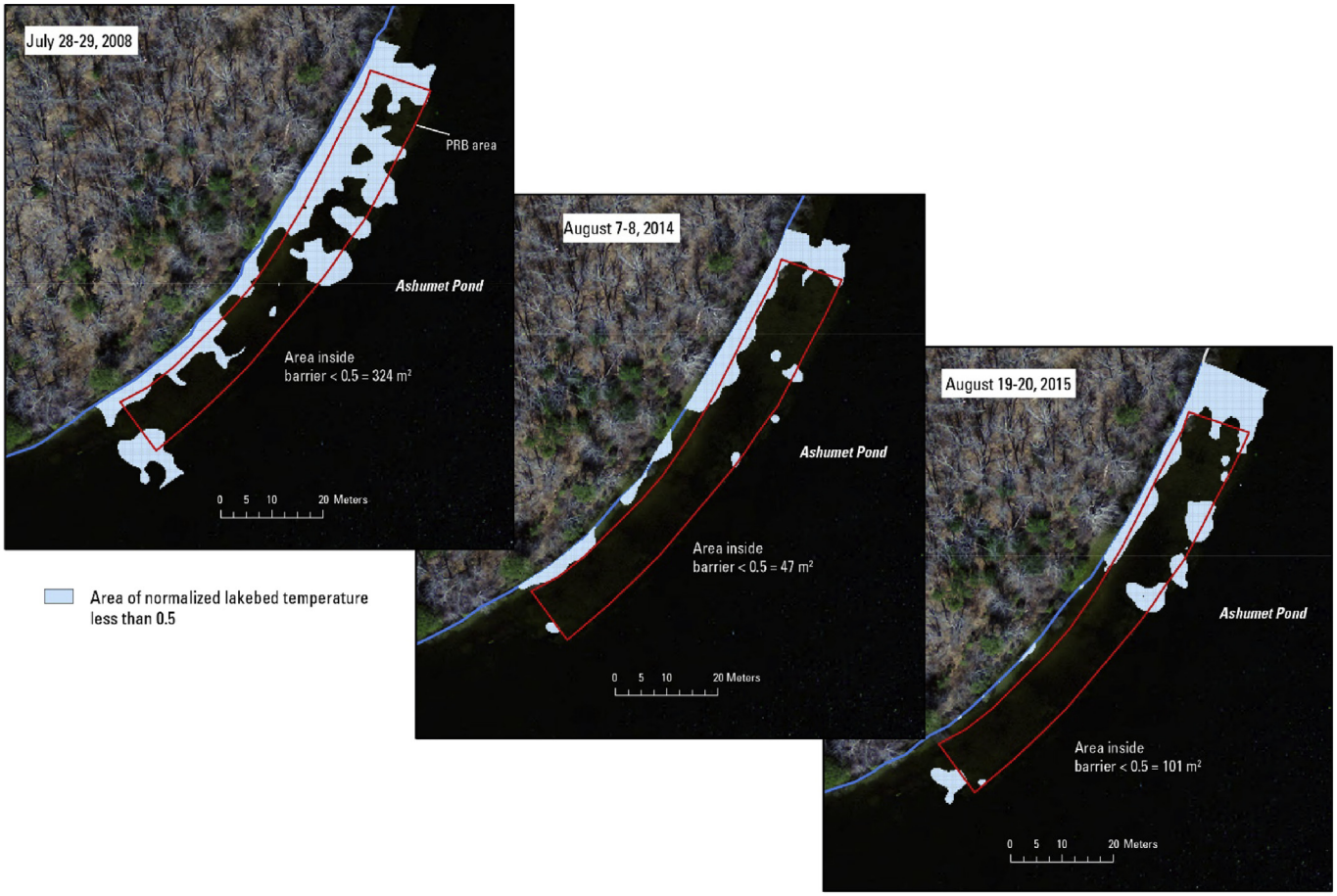

Fig. 5. Maps showing areas of lakebed groundwater with normalized temperature less than 0.5 (strong groundwater upwelling) in the area of a permeable reactive barrier.

the PRB boundary was narrowest.

Spatial patterns in normalized temperatures less than 0.5, a range expected for strong groundwater upwelling, clearly show a reduction in area inside the PRB between the 2008 and the 2014/2015 datasets (Fig. 5). The area of normalized temperature less than 0.5 decreased from 324 m^2 in 2008 to 101 m^2 in 2015. The shape and size of areas of normalized temperature less than 0.5 outside of the PRB did not greatly change during this same period. In the later snapshot rounds, an increased occurrence of difficulty in advancing the thermocouple probe past a crusty layer in the first few centimeters provided qualitative evidence of cementation at the lakebed interface. Also, during all snapshots, evidence of migration of PRB material to areas outside of the PRB boundary (e.g. red staining along shoreline and south of the PRB) was noted.

4.3. Measured seepage patterns (long and short term)

Seepage flux over the PRB area was assessed through direct measurements of seepage through half-barrel meters collected annually over an 11-year span as well as at a sub-daily temporal scale by using modeled vertical temperature profiles.

As described by McCobb et al. (2009a), seepage rates from pairs of meters at sites 2, 3, and 4 (referred to as 2A/B, 3A/B, and 4A/B, respectively) inside the PRB boundary are inversely proportional to distance from shore (Fig. 6). Mean seepage rates over the 11-year period at 1.4, 5.9, and 9.6 m from the shoreward boundary of the PRB were 0.43, 0.27, and 0.12 md^{-1}, respectively. Long-term seepage measurements generally show a declining trend throughout the period with only slight variations related to change in lake stage. The seepage rates decreased on average by 0.021 md^{-1} (or about 4.5 percent) annually over this period for the six meters inside the PRB area.

Annual mean seepage outside the barrier at site 1A/B ranged from 0.22 to 0.84 md^{-1} over the 11-year period. Consistent differences in seepage flux between the two closely spaced meters reflect local heterogeneity at the lakebed. Seepage fluxes through 2011 responded inversely to lake-stage changes, with increasing surface-water depth resulting in decreasing flux; after 2011, however, an apparent positive relation to lake stage was established at some seepage meters. Abundant red iron precipitation on the lakebed is present in this area providing direct evidence that PRB material has migrated outside of the treatment area over time.

In a comparison of mean seepage rates outside of the PRB (site 1) during periods with similar lake stages in 2005 and 2012 (0.02 m difference), mean seepage decreased by 0.13 md^{-1} (or 22 percent). For that same period inside the PRB, mean seepage over all six meters decreased by an average of 0.22 md^{-1} (or 62 percent). Similar declines in seepage were recorded between the 2008 and 2015 measurement sets, which also were made during periods with similar lake stages. Slight declines in seepage over time outside of the PRB could be the result of gradual movement and re-deposition of iron material from the PRB.

In 2015, shorter term (sub-daily) patterns in seepage inside the PRB boundary were assessed using vertical temperature profilers at seven locations chosen to span the general range of bed temperatures measured during the 2015 S-I-T thermal mapping (Fig. 3). The

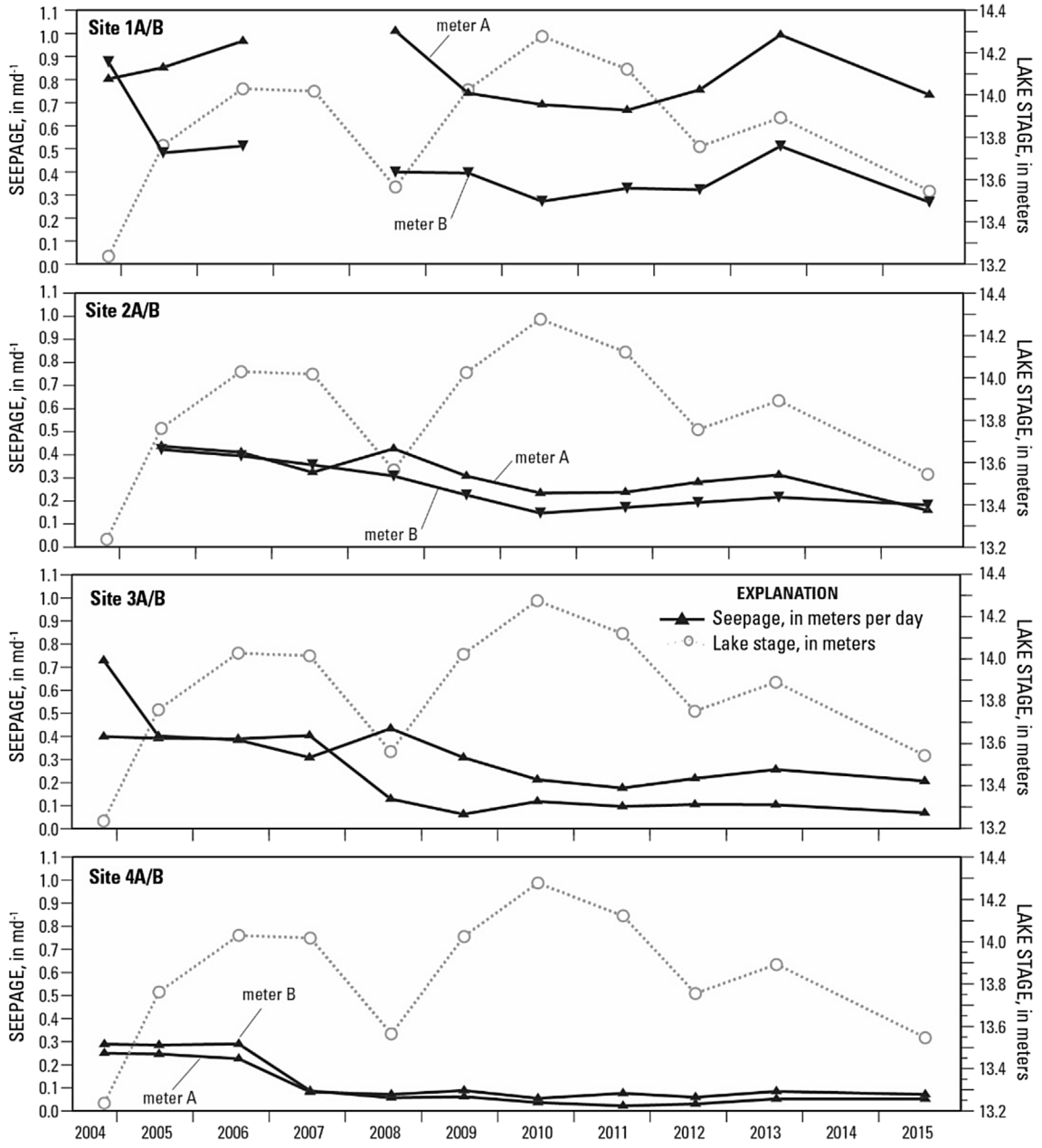

Fig. 6. Water flux at permanent seepage meters installed in and near the permeable reactive barrier, November 2004-August 2015. Locations of seepage meter pairs shown on Fig. 1. Site 1A/B is located outside the PRB; sites 2,3, and 4 are located inside the PRB at 1.4,5.9, and 9.6 m from the shoreward PRB boundary, respectively.

saturated thermal diffusivity, K_e, was evaluated with the Luce et al. (2013) analytical method for location S3 by using diurnal temperature signal time series from four lake-bed depths. The geometric mean of K_e over all possible adjacent depth pairs (e.g. 0.01–0.04 m, 0.04–0.07 m, 0.07–0.011 m) is 0.13 m^2d^{-1} with an arithmetic standard deviation of 0.03 m^2d^{-1}; this reasonably stable mean value was used to optimize the analytical models of vertical seepage flux for all seven locations.

Thermal time series at locations S1 and S4 indicated poor physical coupling between the profiler and bed sediments, and possibly preferential flow along the profiler housing, so these locations were excluded from final seepage flux modeling. For these two locations preliminary VFLUX models indicated downward water movement, yet physical seepage measurements, measured negative thermal gradients with depth, and the geologic setting (upgradient side of flow-through kettle lake) all indicated seepage that should be upward in direction. The remaining five locations show mean values that range from 0.39 to 1.15 md^{-1}, with stronger fluxes generally related to colder bed survey temperatures (Table 3). The temporal variability observed with the vertical temperature profilers compares well with previous measurements of seepage made by using an automated seepage meter within 20–30 m of the PRB that range between 0.25 and 0.50 md^{-1} (Rosenberry et al., 2013). Physical seepage meter measurements were possible at all locations except for S7 where the water depth was too shallow, and all indicated upward water movement. Mean seepage meter measurements are always less than their mean temperature profiler-based counterparts. Location S3 has the lowest mean flux from both methods, indicating that this location was most appropriate for the in-situ evaluation of K_e discussed

Table 3
Mean vertical seepage flux by seepage meter and temperature profiling at seven locations in the PRB area. Locations of temporary seepage sites shown in Fig. 3. [n/a, seepage not measured; —, excluded from flux modeling]

Location	Bed temp (°C) at 0.1 m	Mean vertical seepage flux (m/d)			
		Measured seepage meter	std. dev.	Modeled temperature profiler	std. dev.
S1	29.10	0.14	0.05	—	—
S2	17.90	0.21	0.06	1.15	0.15
S3	22.30	0.05	0.04	0.39	0.09
S4	24.40	0.20	0.06	—	—
S5	29.10	0.27	0.06	0.63	0.09
S6	17.50	0.62	0.23	0.69	0.08
S7	17.50	n/a	n/a	0.81	0.06

above. The temporal patterns of temperature profiler-based seepage show some systematic variation that does not seem to be directly tied to changes in local lake stage (Fig. 7).

5. Discussion

The interpretation of repeated temperature and vertical seepage measurements at the GW/SW interface can be used to evaluate the long-term efficacy of the PRB remediation from a hydraulic flow perspective.

5.1. Groundwater seepage patterns over time by using point and spatially distributed methodology

At the Ashumet Pond PRB, where changes in seepage rates were expected based on previous laboratory observations of pore clogging in PRB material, it is apparent through direct point measurements of seepage, the FO-DTS survey, and S-I-T mapping from the thermal probing data within the PRB that the observed declines over time in seepage are indications of biogeochemical changes in the lakebed sediments as the PRB ages.

Declining water flux through the PRB over time is shown through direct seepage measurements in paired meters emplaced in the ZVI mixture during installation of the PRB. However, seepage meters used once a year to obtain point measurements do not capture the dynamic nature of seepage as it relates to shoreline position over time (changing lake stage) and possibly sub-yearly variations in GW/SW exchange. The position of these point measurements and, in particular, distance from shore can dictate the observed magnitude of seepage through the lakebed. Seepage in homogeneous systems typically responds to changes in lake stage and resulting shoreline position. In the case of this study, where permanent meters were set at fixed locations on the lake bottom, not only is water flux declining over time, but seepage response to stage changes inside the PRB is muted, suggesting a restricted hydraulic connection between the shallow PRB sediments and the deeper untreated sediments.

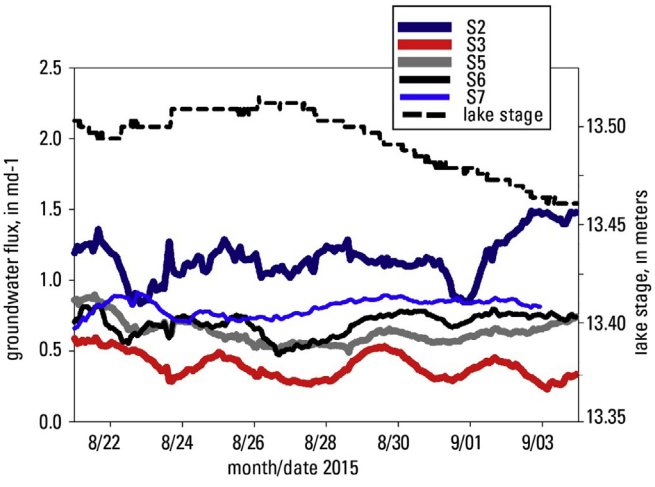

Fig. 7. Short-term seepage patterns derived from vertical bed temperature time series; local lake stage elevation is also depicted.

The S-I-T mapping is a powerful tool for showing spatial patterns of seepage by using temperature as a proxy that reflects the combined characteristics of the lakebed sediments and the local hydraulic gradient. These characteristics result in discrete zones of strong seepage reflecting naturally occurring permeable zones—similar to those described in a nearby stream by Rosenberry et al. (2016)—as well as zones of strong seepage created or enhanced by the PRB construction process. A well-sorted PRB mixture by nature of the installation process should have initially removed shallow heterogeneities over the PRB area; therefore, shallow temperature variations over the PRB should represent spatial changes in the deeper, local hydraulic gradient field. Over time, changes in the spatial temperature patterns should additionally reflect the changing permeability of the lakebed sediments in the area of the PRB. In the earliest thermal mapping snapshots made during this study, the uneven distribution of seepage—both strong advection and conduction zones—is evident and includes zones of enhanced seepage at offshore topographical lows created during installation. In the 2014 and 2015 snapshots, the enhanced manmade zones remain while the uneven temperature distribution over the PRB is less pronounced as bed sediment properties evolve. The S-I-T mapping techniques provide insight into these complexities and are an effective approach for repeatable, long-term monitoring.

The dynamic nature of groundwater exchange reflected in the short-term vertical fluid-flux modeling needs to be considered when comparing measured and modeled point seepage as well as comparing and upscaling snapshot thermal measurements over large areas (Fig. 7). Comparisons of seepage values derived from the vertical bed temperature time series and co-located direct seepage measurements show significant differences—as great as five times higher at thermal profilers—that can be explained based on temporal and spatial differences in the methodologies (Table 3). The modeled seepage fluxes represent mean values averaged over a prescribed timeframe whereas the direct seepage measurements represent a mean of many measurements made over a 1–2 h period. Seepage meters cover a constant area (in this case 0.25 m^2) and the vertical profilers are true point measurements that cover over 100 times less area than the seepage meters. Furthermore, the installation of the vertical thermal profilers may have caused preferential flow around the probes in these cemented sediments. Preferential flow around the measurement device would be reduced when using the seepage meters owing to the averaging over a larger bed area. The timing of S-I-T measurements, both seasonally and daily, is critical for meaningful comparisons of differential temperatures over the long term. Field snapshots ideally would be done during periods of annual extreme surface-water temperatures and only limited recent precipitation events, and should be accomplished over a short (hourly) timeframe during which surface-water temperatures are most nearly constant (early morning and early evening).

The combination of contrasts in temperature-based mapping and point-scale seepage is a powerful approach for understanding lakebed exchange and monitoring potential spatial and temporal changes. The S-I-T mapping methodology is spatially comprehensive and can quickly indicate zones of stronger seepage that can be

quantified by establishing an empirical rating curve by using the point-scale methods. Efforts to quantify fluxes over large lakebed areas by upscaling a small number of point measurements of flux over large areas by using thermal mapping must consider the dynamic system as it relates to timing as discussed by Irvine and Lautz (2015). The distribution of these point measurements should span the largest range of seepage rates to develop the most complete rating curve. Blind siting of point measurements at various points in time and space, even if many points are used, would be labor and time intensive and not provide the complete spatial understanding that is realized by using S-I-T mapping.

5.2. Implications for permeable reactive barrier hydraulic performance

Passive treatment at the GW/SW interface for contaminants such as nutrients and metals is becoming more widespread. For example, wood chips as a PRB reactive media are being used at and near the interface as a source of carbon to promote denitrification in coastal settings (Hiller et al., 2015). These passive systems take advantage of natural groundwater flow to intercept contaminants at and near its discharge point to a water body. Monitoring these systems near the interface is a feasible approach given the site accessibility and availability of the methods discussed in this report.

For this case study, field evidence of reduced seepage flux over time through the PRB indicates a greater likelihood for increased contaminant mass to enter the surface water untreated either on the shoreward edge of the PRB or around the nearest outside PRB boundary. The abundant and persistent discharge along this boundary is most likely enhanced by hydraulic bypassing of the PRB. Interestingly, high seepage zones, depicted as normalized temperatures <0.5, persisted throughout all datasets during the entire 8-year period of thermal mapping (including FO-DTS) (Fig. 8). These areas of persistent high seepage were detected in only 4.9 percent of the study area, of which only 18 percent is inside the PRB area. These persistent areas of flux over time predominantly occur in areas between the shoreline and the PRB, corresponding to areas of elevated phosphate concentrations reported by McCobb et al. (2009b).

Field evidence of cementation of lakebed sediment was observed with increasing frequency during the study, further corroborating that clogging that could reduce permeability is increasing in the PRB over time. Phillips et al. (2003) reported increases in mineral precipitation, cementation of PRB material, and iron oxidation when comparing cores collected only 15 and 30 months after ZVI PRB installation. Examination of cores from the lake-bottom PRB with tools such as X-ray diffraction and scanning electronic microscopy would be needed to confirm mineralogical changes to the sediments over time.

Although this study focuses on evidence for the loss of permeability through the PRB obtained by using hydrologic field observations, previous studies indicated that reactivity of the ZVI material is likely the most probable factor that limits longevity of the PRB (Henderson and Demond, 2007). Recent (2015) samples collected within the Ashumet Pond PRB show that little or no phosphate is present in the upper portions of the PRB near the plume's discharge point at the lakebed. It is unclear if the lack of phosphate in PRB effluent is caused by ZVI reactions as designed or evidence of contaminant mass bypassing the PRB.

6. Conclusions and considerations for remediation and monitoring at the lakebed interface

This paper presented the use of a combination of practical temperature and seepage field measurements to efficiently assess spatial and temporal groundwater discharge patterns through a lakebed area containing a ZVI PRB. The techniques discussed demonstrate to environmental managers considering horizontal barriers at the GW/SW interface that fairly simple and inexpensive methods can provide initial reconnaissance of sand and gravel lakebed/streambed seepage conditions that can be repeated over longer timeframes. For the Ashumet Pond case, FO-DTS and S-I-T thermal mapping qualitatively showed uneven distributions of seepage across the lakebed and highlighted zones of rapid seepage nearest the shoreline and along the outer boundaries of the PRB. When evaluating the geochemical viability of a PRB for its design life—in this case 20 years—these preferential patterns of discharge will need to be considered. Modeling of short-term vertical temperature profilers was used to quantify seepage in low and high temperature zones over the lakebed and demonstrated the dynamic nature of lakebed seepage. The increase of lakebed temperatures in the area of the PRB, declines in direct seepage measured through traditional seepage meters installed in the PRB, and the increase in cementation of the lakebed surface over time support the conclusion that permeability of the PRB is declining over time.

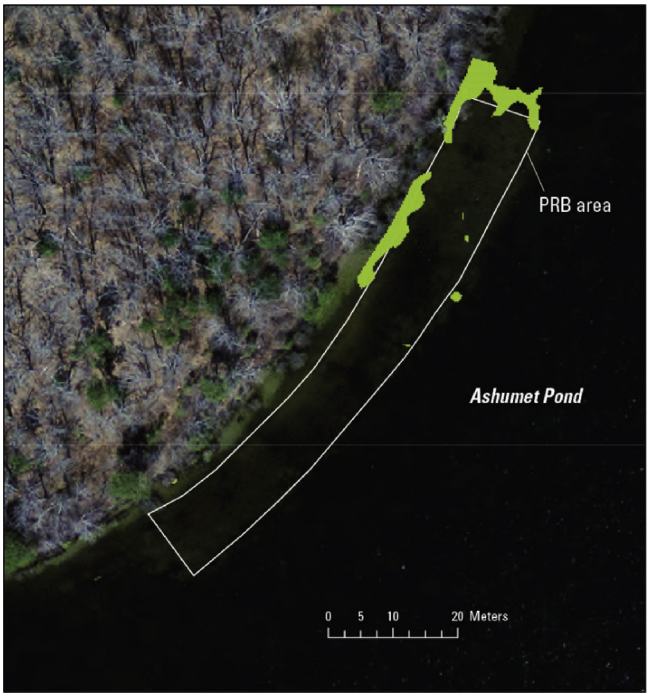

Fig. 8. Areas of persistent strong groundwater discharge over an 8-year period (2007–2015).

The S-I-T techniques repeated over a period of eight years revealed the presence of persistent, rapid seepage zones. Given these long-term persistent zones, remediation managers should consider applying these reconnaissance tools recurrently to identify persistent zones and focus future treatment modifications on small areas of potentially high contaminant mass flux rather than targeting highest concentrations over large treatment areas. An optimized treatment approach targeting high seepage, high concentration zones could significantly reduce remediation costs and environmental disturbance to the sensitive lakebed zone.

Acknowledgments

This study was funded by the Air Force Civil Engineer Center (AFCEC) and the U.S. Geological Survey Toxic Substances Hydrology

Program. Additionally, thermal profiler analysis was supported by Department of Energy grant DE-SC0016412. The authors recognize the many scientists and students who helped during the field surveys including Gillian Pirolli, Robert Hull, Stephen Lukas, and Wesley Johnson. Any use of trade, firm, or product names is for descriptive purposes only and does not imply endorsement by the U.S. Government.

References

Air Force Center for Environmental Excellence, 1997. Draft Ecological Quarterly Data Summery Report.

Anderson, M.P., 2005. Heat as a ground water tracer. Ground Water 43, 951–968. https://doi.org/10.1111/j.1745-6584.2005.00052.x.

Banks, E.W., Shanafield, M.A., Cook, P.G., 2014. Induced temperature gradients to examine groundwater flowpaths in open boreholes. Groundwater 52, 943–951. https://doi.org/10.1111/gwat.12157.

Bredehoeft, J.D., Papadopulos, I.S., 1965. Rates of vertical groundwater movement estimated from the Earth's thermal profile. Water Resour. Res. 1, 325–328. https://doi.org/10.1029/WR001i002p00325.

Briggs, M.A., Buckley, S.F., Bagtzoglou, A.C., Werkema, D.D., Lane, J.W., 2016. Actively heated high-resolution fiber-optic-distributed temperature sensing to quantify streambed flow dynamics in zones of strong groundwater upwelling. Water Resour. Res. 52, 5179–5194. https://doi.org/10.1002/2015WR018219.

Briggs, M.A., Lautz, L.K., Buckley, S.F., Lane, J.W., 2014. Practical limitations on the use of diurnal temperature signals to quantify groundwater upwelling. J. Hydrol. 519 (Part), 1739–1751. https://doi.org/https://doi.org/10.1016/j.jhydrol.2014.09.030.

Briggs, M.A., Lautz, L.K., McKenzie, J.M., Gordon, R.P., Hare, D.K., 2012. Using high-resolution distributed temperature sensing to quantify spatial and temporal variability in vertical hyporheic flux. Water Resour. Res. 48 n/a–n/a. https://doi.org/10.1029/2011WR011227.

Carr, M.R., Winter, T.C., 1980. An Annotated Bibliography of Devices Developed for Direct Measurement of Seepage, Open-file Report.

Carslaw, H.S., Jaeger, J.C., 1959. Conduction of Heat in Solids, Oxford, second ed. Clarendon Press.

Conant, B., 2004. Delineating and quantifying ground water discharge zones using streambed temperatures. Ground Water 42, 243–257. https://doi.org/10.1111/j.1745-6584.2004.tb02671.x.

Constantz, J., 2008. Heat as a tracer to determine streambed water exchanges. Water Resour. Res. 44 n/a–n/a. https://doi.org/10.1029/2008WR006996.

Constantz, J., Cox, M.H., Su, G.W., 2003. Comparison of heat and bromide as ground water tracers near streams. Ground Water 41, 647–656. https://doi.org/10.1111/j.1745-6584.2003.tb02403.x.

Gordon, R.P., Lautz, L.K., Daniluk, T.L., 2013. Spatial patterns of hyporheic exchange and biogeochemical cycling around cross-vane restoration structures: implications for stream restoration design. Water Resour. Res. 49, 2040–2055. https://doi.org/10.1002/wrcr.20185.

Goto, S., Yamano, M., Kinoshita, M., 2005. Thermal response of sediment with vertical fluid flow to periodic temperature variation at the surface. J. Geophys. Res. Solid Earth 110 n/a–n/a. https://doi.org/10.1029/2004JB003419.

Gu, B., Phelps, T.J., Liang, L., Dickey, M.J., Roh, Y., Kinsall, B.L., Palumbo, A.V., Jacobs, G.K., 1999. Biogeochemical dynamics in zero-valent iron Columns: implications for permeable reactive barriers. Environ. Sci. Technol. 33, 2170–2177. https://doi.org/10.1021/es981077e.

Harvey, J.W., Wagner, B.J., Bencala, K.E., 1996. Evaluating the reliability of the stream tracer approach to characterize stream-subsurface water exchange. Water Resour. Res. 32, 2441–2451. https://doi.org/10.1029/96WR01268.

Hatch, C.E., Fisher, A.T., Revenaugh, J.S., Constantz, J., Ruehl, C., 2006. Quantifying surface water–groundwater interactions using time series analysis of streambed thermal records: method development. Water Resour. Res. 42 n/a–n/a. https://doi.org/10.1029/2005WR004787.

Healy, R.W., Ronan, A.D., 1996. Documentation of Computer Program VS2Dh for Simulation of Energy Transport in Variably Saturated Porous media; Modification of the US Geological Survey's Computer Program VS2DT, Water-resources Investigations Report.

Healy, R.W., Winter, T.C., LaBaugh, J.W., Franke, O.L., 2007. Water budgets: foundations for effective water-resources and environmental management. U.S. Geol. Surv. Circ. 1308, 90.

Henderson, A.D., Demond, A.H., 2007. Long-term performance of zero-valent iron permeable reactive barriers: a critical review. Environ. Eng. Sci. 24, 401–423. https://doi.org/10.1089/ees.2006.0071.

Henderson, R.D., Day-Lewis, F.D., Harvey, C.F., 2009. Investigation of aquifer-estuary interaction using wavelet analysis of fiber-optic temperature data. Geophys. Res. Lett. 36 n/a–n/a. https://doi.org/10.1029/2008GL036926.

Hiller, K.A., Foreman, K.H., Weisman, D., Bowen, J.L., 2015. Permeable reactive barriers designed to mitigate eutrophication alter bacterial community composition and aquifer redox conditions. Appl. Environ. Microbiol. 81, 7114–7124. https://doi.org/10.1128/AEM.01986-15.

Irvine, D.J., Briggs, M.A., Cartwright, I., Scruggs, C.R., Lautz, L.K., 2017a. Improved vertical streambed flux estimation using multiple diurnal temperature methods in series. Groundwater 55, 73–80. https://doi.org/10.1111/gwat.12436.

Irvine, D.J., Briggs, M.A., Lautz, L.K., Gordon, R.P., McKenzie, J.M., Cartwright, I., 2017b. Using diurnal temperature signals to infer vertical groundwater-surface water exchange. Groundwater 55, 10–26. https://doi.org/10.1111/gwat.12459.

Irvine, D.J., Lautz, L.K., 2015. High resolution mapping of hyporheic fluxes using streambed temperatures: recommendations and limitations. J. Hydrol. 524, 137–146. https://doi.org/https://doi.org/10.1016/j.jhydrol.2015.02.030.

Irvine, D.J., Lautz, L.K., Briggs, M.A., Gordon, R.P., McKenzie, J.M., 2015. Experimental evaluation of the applicability of phase, amplitude, and combined methods to determine water flux and thermal diffusivity from temperature time series using {VFLUX} 2. J. Hydrol. 531 (Part), 728–737. https://doi.org/https://doi.org/10.1016/j.jhydrol.2015.10.054.

Kalbus, E., Reinstorf, F., Schirmer, M., 2006. Measuring methods for groundwater – surface water interactions: a review. Hydrol. Earth Syst. Sci. 10, 873–887. https://doi.org/10.5194/hess-10-873-2006.

Kamolpornwijit, W., Liang, L., West, O.R., Moline, G.R., Sullivan, A.B., 2003. Preferential flow path development and its influence on long-term PRB performance: column study. J. Contam. Hydrol. 66, 161–178. https://doi.org/. https://doi.org/10.1016/S0169-7722(03)00031-7.

Kazmierczak, J., Müller, S., Nilsson, B., Postma, D., Czekaj, J., Sebok, E., Jessen, S., Karan, S., Stenvig Jensen, C., Edelvang, K., Engesgaard, P., 2016. Groundwater flow and heterogeneous discharge into a seepage lake: combined use of physical methods and hydrochemical tracers. Water Resour. Res. 52, 9109–9130. https://doi.org/10.1002/2016WR019326.

Koch, F.W., Voytek, E.B., Day-Lewis, F.D., Healy, R., Briggs, M.A., Lane, J.W., Werkema, D., 2016. 1DTempPro V2: new features for inferring groundwater/surface-water exchange. Groundwater 54, 434–439. https://doi.org/10.1111/gwat.12369.

Lautz, L.K., Ribaudo, R.E., 2012. Scaling up point-in-space heat tracing of seepage flux using bed temperatures as a quantitative proxy. Hydrogeol. J. 20, 1223–1238. https://doi.org/10.1007/s10040-012-0870-2.

Lee, D.R., 1977. A device for measuring seepage flux in lakes and estuaries. Limnol. Oceanogr. 22, 140–147. https://doi.org/10.4319/lo.1977.22.1.0140.

Lee, D.R., Cherry, J.A., 1978. A field exercise on groundwater flow using seepage meters and mini-piezometers. J. Geol. Educ. 27, 6–10.

Li, L., Benson, C.H., Lawson, E.M., 2005. Impact of mineral fouling on hydraulic behavior of permeable reactive barriers. Ground Water 43, 582–596. https://doi.org/10.1111/j.1745-6584.2005.0042.x.

Liang, L., Sullivan, A.B., West, O.R., Moline, G.R., Kamolpornwijit, W., 2003. Predicting the precipitation of mineral phases in permeable reactive barriers. Environ. Eng. Sci. 20, 635–653. https://doi.org/10.1089/109287503770736159.

Lowry, C.S., Walker, J.F., Hunt, R.J., Anderson, M.P., 2007. Identifying spatial variability of groundwater discharge in a wetland stream using a distributed temperature sensor. Water Resour. Res. 43 n/a–n/a. https://doi.org/10.1029/2007WR006145.

Luce, C.H., Tonina, D., Gariglio, F., Applebee, R., 2013. Solutions for the diurnally forced advection-diffusion equation to estimate bulk fluid velocity and diffusivity in streambeds from temperature time series. Water Resour. Res. 49, 488–506. https://doi.org/10.1029/2012WR012380.

Mamer, E.A., Lowry, C.S., 2013. Locating and quantifying spatially distributed groundwater/surface water interactions using temperature signals with paired fiber-optic cables. Water Resour. Res. 49, 7670–7680. https://doi.org/10.1002/2013WR014235.

McBride, M.S., Pfannkuch, H.O., 1975. Distribution of seepage within lake beds. J. Res. U. S. Geol. Surv. 3, 505–512.

McCobb, T.D., Briggs, M.A., Leblanc, D.R., Day-Lewis, F.D., Johnson, C.D., 2018. Temperature and Seepage Data from a Lake-Bottom Permeable Reactive Barrier. Ashumet Pond, Falmouth, MA, 2004-2015 [WWW Document]. U.S. Geol. Surv. Data Release. https://doi.org/10.5066/F78914ZS.

McCobb, T.D., LeBlanc, D.R., Massey, A.J., 2009a. Monitoring the removal of phosphate from ground water discharging through a pond-bottom permeable reactive barrier. Ground Water Monit. Remediat. 29, 43–55. https://doi.org/10.1111/j.1745-6592.2009.01235.x.

McCobb, T.D., LeBlanc, D.R., Parsons, L.A., Blount, J.G., 2009b. Distribution of Treated-wastewater Constituents in Pore Water at a Pond-bottom Reactive Barrier, Cape Cod, Massachusetts, U.S. Geological Survey Scientific Investigations Map 3078.

McCobb, T.D., LeBlanc, D.R., Walter, D.A., Hess, K.M., Kent, D.B., Smith, R.L., 2003. Phosphorus in a Ground-water Contaminant Plume Discharging to Ashumet Pond, Cape Cod, Massachusetts, 1999, Water-resources Investigations Report.

Murdoch, L.C., Kelly, S.E., 2003. Factors affecting the performance of conventional seepage meters. Water Resour. Res. 39 (1163). https://doi.org/10.1029/2002WR001347.

Phillips, D.H., Nooten, T., Van Bastiaens, L., Russell, M.I., Dickson, K., Plant, S., Ahad, J.M.E., Newton, T., Elliot, T., Kalin, R.M., 2010. Ten year performance evaluation of a field-scale zero-valent iron permeable reactive barrier installed to remediate trichloroethene contaminated groundwater. Environ. Sci. Technol. 44, 3861–3869. https://doi.org/10.1021/es902737t.

Phillips, D.H., Watson, D.B., Roh, Y., Gu, B., 2003. Mineralogical characteristics and transformations during long-term operation of a zerovalent iron reactive barrier. J. Environ. Qual. 32, 2033–2045. https://doi.org/10.2134/jeq2003.2033.

Rau, G.C., Andersen, M.S., McCallum, A.M., Acworth, R.I., 2010. Analytical methods that use natural heat as a tracer to quantify surface water-groundwater exchange, evaluated using field temperature records. Hydrogeol. J. v. 18, 1093-1110–2010 v.18 no.5 https://doi.org/10.1007/s10040-010-0586-0.

Rau, G.C., Andersen, M.S., McCallum, A.M., Roshan, H., Acworth, R.I., 2014. Heat as a

tracer to quantify water flow in near-surface sediments. Earth Sci. Rev. 129, 40–58. https://doi.org/10.1016/j.earscirev.2013.10.015.
Read, T., Bour, O., Bense, V., Le Borgne, T., Goderniaux, P., Klepikova, M.V., Hochreutener, R., Lavenant, N., Boschero, V., 2013. Characterizing groundwater flow and heat transport in fractured rock using fiber-optic distributed temperature sensing. Geophys. Res. Lett. 40, 2055–2059. https://doi.org/10.1002/grl.50397.
Rosenberry, D.O., Briggs, M.A., Delin, G., Hare, D.K., 2016. Combined use of thermal methods and seepage meters to efficiently locate, quantify, and monitor focused groundwater discharge to a sand-bed stream. Water Resour. Res. 52, 4486–4503. https://doi.org/10.1002/2016WR018808.
Rosenberry, D.O., LaBaugh, J.W., 2008. Field Techniques for Estimating Water Fluxes Between Surface Water and Ground Water, Techniques and Methods.
Rosenberry, D.O., Lewandowski, J., Meinikmann, K., Nützmann, G., 2015. Groundwater - the disregarded component in lake water and nutrient budgets. Part 1: effects of groundwater on hydrology. Hydrol. Process. 29, 2895–2921. https://doi.org/10.1002/hyp.10403.
Rosenberry, D.O., Morin, R.H., 2004. Use of an electromagnetic seepage meter to investigate temporal variability in lake seepage. Ground Water 42, 68–77. https://doi.org/10.1111/j.1745-6584.2004.tb02451.x.
Rosenberry, D.O., Sheibley, R.W., Cox, S.E., Simonds, F.W., Naftz, D.L., 2013. Temporal variability of exchange between groundwater and surface water based on high-frequency direct measurements of seepage at the sediment-water interface. Water Resour. Res. 49, 2975–2986. https://doi.org/10.1002/wrcr.20198.
Sass, B.M., Gavaskar, T., Gupta, N., Yoon, W., Hicks, J.E., O'Dwyer, D., Reeter, C., 1998. Evaluating the moffett field permeable barrier using groundwater monitoring and geochemical modeling. In: Wickramanayake, G.B., Hinchee, R.E. (Eds.), Designing and Applying Treatment Technologies, Remediation of Chlorinated and Recalcitrant Compounds. Battelle Publishers, Columbus, OH, pp. 169–175.
Savoie, J.G., LeBlanc, D.R., Fairchild, G.M., Smith, R.L., Kent, D.B., Barber, L.B., Repert, D.A., Hart, C.P., Keefe, S.H., Parsons, L.A., 2012. Groundwater-quality Data for a Treated-wastewater Plume Near the Massachusetts Military Reservation, Ashumet Valley, Cape Cod, Massachusetts, 2006-08. Data Series, Reston, VA.
Sebok, E., Duque, C., Kazmierczak, J., Engesgaard, P., Nilsson, B., Karan, S., Frandsen, M., 2013. High-resolution distributed temperature sensing to detect seasonal groundwater discharge into Lake Væng. Den. Water Resour. Res. 49, 5355–5368. https://doi.org/10.1002/wrcr.20436.
Selker, J.S., Thévenaz, L., Huwald, H., Mallet, A., Luxemburg, W., van de Giesen, N., Stejskal, M., Zeman, J., Westhoff, M., Parlange, M.B., 2006. Distributed fiber-optic temperature sensing for hydrologic systems. Water Resour. Res. 42 n/a–n/a. https://doi.org/10.1029/2006WR005326.
Slater, L.D., Ntarlagiannis, D., Day-Lewis, F.D., Mwakanyamale, K., Versteeg, R.J., Ward, A., Strickland, C., Johnson, C.D., Lane, J.W., 2010. Use of electrical imaging and distributed temperature sensing methods to characterize surface water–groundwater exchange regulating uranium transport at the Hanford 300 Area, Washington. Water Resour. Res. 46. https://doi.org/10.1029/2010WR009110.
Stonestrom, D.A., Constantz, J., 2003. Heat as a Tool for Studying the Movement of Ground Water Near Streams, Circular.
Su, C., Puls, R.W., 2003. In situ remediation of arsenic in simulated groundwater using zerovalent iron: laboratory column tests on combined effects of phosphate and silicate. Environ. Sci. Technol. 37, 2582–2587. https://doi.org/10.1021/es026351q.
Tyler, S.W., Selker, J.S., Hausner, M.B., Hatch, C.E., Torgersen, T., Thodal, C.E., Schladow, S.G., 2009. Environmental temperature sensing using Raman spectra DTS fiber-optic methods. Water Resour. Res. 45 n/a–n/a. https://doi.org/10.1029/2008WR007052.
Voss, C.I., 1984. A Finite-element Simulation Model for Saturated-unsaturated, Fluid-density-dependent Ground-water Flow with Energy Transport or Chemically- Reactive Single-species Solute Transport, Water-resources Investigations Report.
Westhoff, M.C., Savenije, H.H.G., Luxemburg, W.M.J., Stelling, G.S., van de Giesen, N.C., Selker, J.S., Pfister, L., Uhlenbrook, S., 2007. A distributed stream temperature model using high resolution temperature observations. Hydrol. Earth Syst. Sci. 11, 1469–1480. https://doi.org/10.5194/hess-11-1469-2007.
Wilkin, R.T., Puls, R.W., Sewell, G.W., 2003. Long-term performance of permeable reactive barriers using zero-valent iron: geochemical and microbiological effects. Ground Water 41, 493–503. https://doi.org/10.1111/j.1745-6584.2003.tb02383.x.